SLAC-PUB-1176

A MODEL FOR pp → pX INCLUSIVE REACTION AT SMALL MOMENTUM TRANSFERS

A. Capella, H. Högaasen, and V. Rittenberg

ERRATA

P. 12, line 1:	change ref. 15 to ref. 16
P. 12, Eq. (22):	last part of equation should read $g^R_{PP}(t)\, G^2_P(t)\, s^{\nu-3/2}$
P. 12, Eq. (23):	change $0.25\, e^{11.9t}$ to read $250\, e^{11.9t}$
P. 13, line 8 from the bottom:	change Figs. 2a and 2b to read Figs. 3a and 3b
P. 14, line 9:	change Fig. 2b to read Fig. 2
P. 14, line 19:	change M = 1.78 GeV to read M = 1.6 GeV
P. 14, line 13:	change Fig. 3 to read Fig. 2
P. 15, line 2:	change Fig. 3 to read Fig. 2
P. 15, line 3 under heading Conclusion:	However, following ref. 2, an exponential term...
P. 20, line 7 in caption 2:	(This amounts to changing the intercept from...
P. 21, line 3 of number 4:	should read ... of Eq. (24)(curve A).

SLAC-PUB-1176
(TH) and (EXP)
January 1973

A MODEL FOR pp → pX INCLUSIVE REACTION AT SMALL MOMENTUM TRANSFERS*

A. Capella†

Stanford Linear Accelerator Center
Stanford University, Stanford, California 94305

H. Högaasen

University of Oslo
Oslo, Norway

V. Rittenberg††

The Rockefeller University
New York, N. Y. 10021

(Submitted to Phys. Rev.)

---

*Work supported in part by the U. S. Atomic Energy Commission.

†On leave from the Laboratoire de Physique Theorique et Particules Elementaires, Orsay.

††On leave from the Tel-Aviv University, Ramat Aviv.

ABSTRACT

The study of the resonant contribution to the finite mass sum rules for the forward Pomeron-proton scattering amplitude obtained from the $pp \rightarrow pX$ spectra for $0.1 < |t| < 0.5$ $(GeV)^2$ suggests that: (a) local duality works nicely for a missing mass larger than 1450 MeV. The nucleon and the 1410 MeV enhancement cooperate in order to saturate the first moment sum rule, (b) there is evidence for a wrong signature fixed pole at J=1 whose residue is exponential in the mass of the Pomeron, (c) the PPR triple Regge term obtained from the finite mass sum rules turns out to be much too small to account for the diffractive part of the proton spectrum at the ISR energies. Reciprocally, if one fits this part of the spectrum with a PPR term, the contribution of such a term at accelerator energies is much larger than the experimental data. These results tend to indicate that most of the diffraction observed at ISR is due to a PPP term.

1. Introduction

The purpose of this paper is to present a simple model which describes the missing mass spectra of the $p(p_a) + p(p_b) \rightarrow p(p_c) + X$ inclusive reaction at small momentum transfer, $|t| \lesssim 1\ (\mathrm{GeV})^2$. (We define $s = (p_a + p_b)^2$, $t = (p_a - p_c)^2$ and $M^2 = (p_a + p_b - p_c)^2$.) The model is essentially a triple Regge model with PPP, PPR, RRP, and RRR terms. We proceed in the following way: First, we determine the arbitrary quantities in the model from a fit of the proton spectrum at $15\ \mathrm{GeV/c} < p_{lab} < 30\ \mathrm{GeV/c}$. More precisely:

(1) The PPR term is obtained from the data in the resonance region ($M < 2.5$ GeV), using the finite mass sum rules (FMSR) and the Harari-Freund two-component duality hypothesis for the Pomeron-proton scattering amplitude. Two important results of this analysis are: (a) the separate contribution of the nucleon pole and the 1410 (Roper) enhancement to the PPR residue, via the FMSR (in the narrow-width approximation), are functions of t very rapidly varying, but the sum of these two contributions is a smooth function of t; (b) the FMSR is roughly independent of the mass cut $\bar{M}$, provided the cut is done after the 1410 enhancement.

(2) The RRP and RRR terms are determined from a fit to the above data outside the resonance region ($M > 2.5$ GeV).[1] We furthermore constrain the RRP and RRR residues in such a way that the sum of these two terms approximately reproduces (at least in an average way) the background under the resonances. This ensures that the complete FMSR is satisfied and, as a consequence, that the fit above extrapolates well into the resonance region. Apart from achieving this goal, an important result of our analysis, already obtained in ref. 2, is the following: The

RRP term has to be replaced by the simple empirical expression:

$$S\left(t, \frac{M^2}{s}\right) = \frac{\beta(t)}{\pi} e^{\left(c_1 - c_2 t\right)\frac{M^2}{s}} \qquad (1)$$

where c_1 and c_2 are constants. The physical interpretation of Eq. (1) is yet obscure but it is a fact of life that such a term is required by the experimental data for $\frac{s}{M^2} < 5\text{-}10$ (where the validity of the triple Regge approach is, of course, rather dubious). Since for $t = 0$, in the expansion of S in powers of $\frac{M^2}{s}$, the first term is a constant, one can consider that S represents approximately the sum of the contributions of the RRP term and its daughters. The fact that they pile-up in a simple form is a mystery, together with the observation that nonleading contributions do not seem to be important for the RRR or PPR terms. It is likely that terms similar to S appear in other inclusive reactions as well,[3] and that their presence is related to the quantum numbers of the $B\bar{C}$ channel alone. Thus if the $B\bar{C}$ channel is exotic (like in the $p\pi^- \rightarrow \pi^+ + X$ reaction), the S term does not seem to be present.

(3) The PPP is assumed to be unimportant at the energies under consideration.

In a second step, we proceed to compare the results of our model with the ISR data at $s = 440$ and 1995 $(GeV)^2$. We find that the agreement is good in the region $s/M^2 < 10$ ($x \sim 1 - M^2/s < 0.9$). In this region, the most important term is, by far, the term $S(t, M^2/s)$. This indicates that the parameterization in Eq. (1) is essentially correct. However, in the diffraction region ($0.9 < x < 1$), our model gives a much too low value for the invariant cross section. Moreover, the energy dependence of the data in this region is such that a PPP term has to be introduced. It turns out that this term accounts for most of the diffraction observed at the ISR.

Let us now describe the model in a more quantitative way. We assume that the differential cross section has the following structure:

$$E_c \frac{d^3\sigma}{dp_c} = T(s,t,M^2) + S\left(t, \frac{M^2}{s}\right) \tag{2}$$

where S is given in Eq. (1), and T can be expressed in terms of the leading contributions of a triple-Regge expansion:

$$T(s,t,M^2) = \frac{1}{\pi s} \sum_{m,n} G_m(t)\, G_n(t) \left(\frac{s}{s_0}\right)^{\alpha_m(t)+\alpha_n(t)} \xi_m\, \xi_n^*\, A_{mn}(t,M^2) \tag{3}$$

A_{mn} is the absorptive part of the forward amplitude for Reggeon proton-Reggeon proton scattering, corresponding to maximum helicity flip in the crossed channel, and ξ_m and ξ_n are the signature factors. For large values of M^2, we have

$$A_{mn} = \sum_k g^k_{m,n}(t) \left(\frac{\nu}{s_0}\right)^{\alpha_k(0) - \alpha_m(t) - \alpha_n(t)} \tag{4}$$

where $\nu = \nu(M) = M^2 - M_p^2 - t$ (M_p is the proton mass).

For simplicity, we assume that the trajectories have the standard form: $\alpha_P(t) \approx 1$, $\alpha_R(t) = 0.5 + t$, $s_0 = 1\ (\text{GeV})^2$. ($\alpha_P(t)$ and $\alpha_R(t)$ represent the Pomeron and the normal trajectories.)

We thus write (neglecting mixed terms in which $\alpha_m \neq \alpha_n$):

$$T = \frac{1}{\pi}\left[s A_{PP}(t,M^2)\, G_P^2(t) + s^{2t} A_{RR}(t,M^2)\, G_R^2(t)\right] \tag{5}$$

where $G_P^4(t) \approx \left(\frac{d\sigma}{dt}\right)_N$. ($\left(\frac{d\sigma}{dt}\right)_N$ is the differential cross section for pp elastic scattering.)

For large values of M^2, we can use the expansion (4):

$$A_{RR} = g^R_{RR}(t)\ \nu^{-0.5-2t} \tag{6}$$

$$A_{PP} = g^P_{PP}(t)\,\nu^{-1} + g^R_{PP}(t)\,\nu^{-3/2} \tag{7}$$

In (6), we have considered only the RRR term, since the RRP contribution was already included in $S(t, M^2)$.

At this stage of the game, we are left with the unknown functions, $\beta(t)$, $g^R_{RR}(t)$, $g^P_{PP}(t)$, $g^R_{PP}(t)$, and constants c_1 and c_2.

In order to determine the function $g^R_{PP}(t)$, in Section 2 we study the finite-mass sum rules (FMSR) and saturate them with diffractively produced resonances. We discuss how duality works for Pomeron-proton scattering, as well as the possible existence of fixed poles.

In Section 3, we use the high missing mass (outside the resonance region) data at 14.2, 19.2, and 24 GeV/c of ref. 4 in order to determine the remaining unknown quantities with the exception of $g^P_{PP}(t)$.[1]

In Section 4, we use the ISR data of $s = 440$ and 1995 $(\text{GeV})^2$, where the eventual contribution of a PPP term ought to appear. We conclude that such a term is indeed present and it is responsible for most of the diffraction observed at the ISR.

Our model gives a simple and quantitative description of all available high-energy ($p_{lab} > 14$ GeV/c) and low-momentum transfer data.

2. Low Missing-Mass Spectrum at $p_{lab} = 24$ GeV/c

The differential cross section $E_c \frac{d^3\sigma}{d^3p_c}$ has the following features: in the small $|t|$ ($|t| < 1(\text{GeV})^2$), small M ($M < 2.5$ GeV), and in the incident energy range ($14.2 < p_{lab} < 30$ GeV/c)[5,6]:

(1) A bump structure in which the N(940) and the N*(1410, 1500, 1690, and 2190) enhancements are observed which, when separated from the background, have a cross section which is roughly energy-independent. When comparison with other reactions is possible (like for the N*(1690) produced in p-p, π-p, k^--p, and $\bar{p}$-p scattering), there is agreement with factorization suggesting that these enhancements are produced through a factorized Pomeron exchange. Thus

$$\left(\frac{d\sigma}{dt}\right)_i = G_P^2(t)\, G_i^2(t) \qquad (i = 940,\ 1410,\ 1500,\ 1690,\ 2190) \tag{8}$$

If the differential cross sections are fit to the exponential form:

$$\left(\frac{d\sigma}{dt}\right)_i = A_i\, e^{b_i t} \tag{9}$$

where $|t| < 0.2\ (\text{GeV})^2$ for N*(1410) and $|t| < 0.9$ for the other enhancements, we get $b_{940} \approx 9(\text{GeV})^{-2}$, $b_{1410} \approx 15$, $b_{1500} \approx b_{1690} \approx b_{2190} \approx 5$. Thus the slope first increases with the mass M and afterward decreases.

The single exponential fit to the data does not describe properly the very small $|t|$ region ($|t| < 0.1$) where $\left(\frac{d\sigma}{dt}\right)_{940}$ has a higher slope,[7] $\left(\frac{d\sigma}{dt}\right)_{1500}$ and $\left(\frac{d\sigma}{dt}\right)_{1690}$ may level off.

(2) At fixed t, the nonresonant background in the mass spectra decreases with the incoming energy.

In this section, we study in detail the problem of enhancements produced by diffraction dissociation using finite mass sum rules (FMSR) and duality[8,9] in

order to determine the unknown residue function $g^R_{PP}(t)$. We use the notation:

$$g^R_{PP}(t) = g(t) \tag{10}$$

(a) First moment FMSR

The first moment FMSR is[10]:

$$\int_0^N d\nu\, \nu \left(A_{PP}(t, M^2) - g(t)\, \nu^{-3/2} \right) = 0 \tag{11}$$

We assume that the resonances build the $\alpha_k(0) = 1/2$ trajectory. This corresponds to the usual Harari-Freund[11] hypothesis. We will also assume that the extrapolation of the Regge term at low values of M^2 has either one of the following two expressions[12]:

$$\lim_{M^2 \to 0} \nu^{-3/2} \longrightarrow \nu^{-3/2} \tag{12a}$$

$$\lim_{M^2 \to 0} \nu^{-3/2} \longrightarrow (\nu M)^{-1} \tag{12b}$$

Using the zero-width approximation, from Eqs. (11) and (12), we get:

$$\frac{1}{2\left[\left(\nu(\bar{M})\right)^{1/2} - \left(\nu(M_p)\right)^{1/2}\right]} \sum_{M_i < \bar{M}} \nu_i G_i^2(t) = g_1(\bar{M}, t) \tag{13a}$$

$$\frac{1}{2(\bar{M} - M_p)} \sum_{M_i < \bar{M}} \nu_i G_i^2(t) = g_2(\bar{M}, t) \tag{13b}$$

where $G_i(t)$ are defined by Eq. (8), $\bar{M}$ is the cut-off mass, and

$$\lim_{\bar{M}\to\infty} g_1(\bar{M}, t) = g_1(t) \tag{14a}$$

$$\lim_{\bar{M}\to\infty} g_2(\bar{M}, t) = g_2(t) \tag{14b}$$

We have saturated the FMSR (13) using the 24-GeV/c data of ref. 5 for N(940) and N*(1400, 1520, 1690). We have left out the 2190-MeV bump because we think that the way the background was extracted gives a too small cross section (see Section 3). We have chosen $\bar{M}$ = 1350, 1450, 1550 and 2000 MeV each enhancement sharing a reasonable range of the M scale.

The two functions $g_1(\bar{M}, t)$ and $g_2(\bar{M}, t)$ as functions of $\bar{M}$ at different fixed t values ($0.1 < |t| < 0.5$) are practically independent of $\bar{M}$ for $\bar{M} > 1450$ MeV although they slightly differ between themselves (see Fig. 1).

(b) Comments on local duality as applied to Pomeron-proton scattering

In order to check how local duality works, we have build the function $g_1^i(t)$ from each resonance separately using:

$$g_1^i(t) \sim \frac{\nu_i \, G_i^2(t)}{2\left[\left(\nu(\bar{M}_i)\right)^{1/2} - \left(\nu(\bar{M}_{i-1})\right)^{1/2}\right]} \tag{15a}$$

[Here $\bar{M}_i$ ($\bar{M}_{i-1}$) denotes the value of $\bar{M}$ immediately above (below) M_i.] As one sees from Fig. 1, the data for the 1520 and 1690 MeV resonances are very close to $g_1(t)$ showing that local duality works nicely. The picture is entirely different for the 1400 enhancement in which case the function g_1^{1400} is different from g_1 and accidentally coincides with it for $|t| \approx 0.14$ $(\text{GeV})^2$; that is why in some pictures of ref. 8 where values of $|t|$ around 0.1 have been considered, the 1400 enhancement looked to be averaged by the Regge curve. In the case of the nucleon the

function $g_1^{940}(t)$ obtained from (15a) differs from $g_1(t)$ obtained from (13a) in the small $|t|$ ($|t| < 0.14$) region (where the 1400 enhancement is present) going too fast to zero as $|t| \to 0$. This seems to be again a qualitative less than a quantitative feature of the data.

However summing up the contributions of the 940 and 1400 one gets a good approximation of $g_1(t)$ (see Fig. 1).

We have repeated the same game with the function $\tilde{g}_2(t)$ using instead of (15a)

$$\frac{\nu_i G_i^2(t)}{2(\bar{M}_i - \bar{M}_{i-1})} \approx g_2^i(t) \tag{15b}$$

The results are shown again in Fig. 1, the functions $g_2(t)$ obtained from the sum of 940 and 1400, from 1520 and 1690 cluster around the $g_2(t)$ function obtained from Eq. (13b).

In order to deal with the unusual behavior of the 1400 enhancement there are, in our opinion, two ways:

(1) The 1400 should not be introduced at all in the FMSR (15) attributing the whole interval up to $\bar{M} = 1450$ MeV to the nucleon alone. In this case however since $\nu_{940}\, G_{940}^2(t) = |t|\, G_{940}^2(t)$ one should expect $g_1(t)$ and $g_2(t)$ to vanish at small $|t|$ at the same rate if local duality works at least qualitatively. Similarly $G_{1500}^2(t)$ and $G_{1690}^2(t)$ should also vanish at $|t| = 0$ at the same rate. This does not seem to be experimentally the case but more careful measurements at $|t| < 0.1$ may give such a picture.

(2) If $g_1(0) \neq 0$ ($g_2(0) \neq 0$) or $g_1(t)$ ($g_2(t)$) tends to zero in a different way than $|t|\, G_{940}^2(t)$, local duality is not verified by the nucleon, its contribution being too small at small $|t|$. However adding the contribution of the 1400 which is large at small $|t|$, the FMSR (11) is saturated but only after $\bar{M} = 1450$ MeV. At larger

$|t|$ ($|t| > 0.15$) the contribution of the nucleon is large enough so that the 1400 has to disappear. Thus, the 1400 is in some sense the partner of the nucleon helping it to satisfy the FMSR at $|t| < 0.15$. The fact that the nucleon plays a special role in the first moment sum rule should not be surprising since, as we shall see it has an unusual behavior in the zeroth order FMSR as well. One can argue that our conclusions are just a result of taking the first moment FMSR and of the importance of the external masses ($\widetilde{M_p^2}$ and t) in the definition of ν. This may be true but we have however to keep in mind that the 1400 enhancement appears only in the $|t| < 0.2$ $(GeV)^2$ region and thus its understanding should be sensitive to the values of the external masses.

(c) Zeroth order finite mass sum rule

We now consider the zeroth order FMSR in order to compute the $R_r(t)$ of the J=1 wrong signature fixed pole using the Schwartz sum rule[13] for the diffractively produced resonances:

$$\int_0^N d\nu \left(A_{PP}(t, M^2) - g(t)\, \nu^{-3/2}\right) = R_r(t) \tag{16}$$

Using again the zero width approximation and the low M^2 extrapolations of the Regge term, (12a) and (12b), we get respectively:

$$\sum_{M_i<\bar{M}} G_i^2(t) = R_r(t) + 2g_1(t)\left[\left(\nu(M_p)\right)^{-1/2} - \left(\nu(\bar{M})\right)^{-1/2}\right] \tag{17a}$$

$$\sum_{M_i<\bar{M}} G_i^2(t) = R_r(t) + \frac{g_2(t)}{M_p \xi}\, \ell n\left[\left(\frac{1+\xi}{1-\xi}\right)\left(\frac{x-\xi}{x+\xi}\right)\right] \tag{17b}$$

where $\xi = \left(1 + \frac{t}{M_p^2}\right)^{1/2}$, $x = \frac{\bar{M}}{M_p}$. Since the functions $g_1(t)$ and $g_2(t)$ are now known functions, from Eq. (17) we can compute $R_r(t)$. Taking $\bar{M} = 1450$, 1550, and

2000 MeV we have checked that the $\bar{M}$ dependence of the left-hand side of Eq. (17) are nicely described by the right-hand side of the same equations and got

$$R_r(t) = 5.4\, e^{4.8\, t}\ (\text{mb})^{1/2}(\text{GeV})^{-1} \qquad (0.1<|t|<0.5) \tag{18a}$$

$$R_r(t) = 7.0\, e^{5.2\, t}$$

A more precise determination of $R_r(t)$ is beyond our means.[14] A very interesting feature of the residue function is its exponential behavior in t.

Since we have not considered the nonresonant contribution to the FMSR (16) the actual residue of the J=1 fixed pole

$$R(t) = R_r(t) + R_n(t) \tag{19}$$

remains unknown ($R_n(t)$ is the contribution of the background which may be negative). In ref. 9 however it was pointed out that $R(t) = 0$ seems very unlikely. The function R(t) can be related to the Pomeron-Pomeron cut contribution in p-p scattering[15], hence the relevance of our results.

(d) The residue function $g^R_{PP}(t)$

The above calculations have been repeated using the experimental results of Ref. 5 at $p_{lab} = 20$ GeV/c, all the qualitative features of our analysis are unchanged and the functions g_1 and g_2 are roughly the same. From now on, we are going to use the parametrization (12a) and therefore we take the residue

function $g^R_{PP}(t) = g_1(t)$.[15] For practical calculations we note that

$$g_1(t) \sim \frac{0.75\ |t|\ G_p^2(t)}{(\nu\,(1.78))^{1/2} - (\nu\,(940))^{1/2}} \quad (|t| > 0.2\ (\text{GeV})^2) \tag{20}$$

with

$$G_p^4(t) = 82\ e^{8.5\ t} \quad . \tag{21}$$

3. High Missing Mass Spectrum at $p_{lab} = 14.2,\ 19.2$ and 24 GeV/c

(a) The high missing mass spectrum

In order to determine the yet unknown residue functions $\gamma(t) = g^R_{RR}(t)\ G^2_R(t)$, $\beta(t)$ and the constants c_1 and c_2, we have considered the experimental data of ref. 3 at 14.2, 19.2, and 24 GeV/c for M values outside the resonance region.

Using (1), (4) - (7), (20), and (21) we have:

$$E_c \frac{d^3\sigma}{dp_c} = \frac{1}{\pi}\left[\frac{\sqrt{s}}{\sqrt{s-4M_p^2}}\left(\frac{\gamma(t)}{s}\left(\frac{s}{M^2}\right)^{1+2t}\nu^{+1/2} + \beta(t)\ e^{(c_1 - c_2 t)\frac{M^2}{s}}\right) + g^R_{PP}(t)\, s\nu^{-3/2}\right] \tag{22}$$

From a best fit to the data we get[17]:

$$\begin{aligned} \gamma(t) &= 79\ e^{0.13\ t} + 0.25\ e^{11.9\ t} \\ \beta(t) &= 13\ e^{6.7\ t + 2.8\ t^2} \\ c_1 &= 7.5\ , \qquad c_2 = 0.25\ . \end{aligned} \tag{23}$$

Equation (22) reproduces very well the data.[18] In order to give a feeling of the quality of the fit, we present in Fig. 2 the 37 mrad data at 24 GeV/c together with the theoretical curve. The experimental points have a 3% error. Notice that at $p_{out} \approx 12$ GeV/c one has $|t| \approx 1\ (\text{GeV})^2$ which is the limit where our parametrization is valid. For smaller angles corresponding to smaller values of $|t|$, the fit is even better.

(b) A model for the nonresonant background at small missing masses

Since we know that the last term in (22) gives an averaged description of the diffractively produced resonances, we have checked if the two first terms in Eq. (22) may describe the nonresonant background in the low missing-mass region. In Figs. 3a and 3b we show the experimental data of ref. 5 for $\theta_{el} = 15$ mrad and 27 mrad at $p_{lab} = 24$ GeV/c together with the predictions of Eq. (22). The "experimental" background which was used to separate the resonances is also shown; the cross sections for these resonances has been used in Section 2.

As one observes, the "theoretical" background (i.e., the sum of the first and second term in Eq. (22)) and the "experimental" background are very close to each other. However, in the region of the 2190 MeV enhancement, although the two backgrounds are close to each other, using the theoretical background to separate the enhancement would yield a substantially higher cross section due to the smallness of the resonance contribution (see Section 2).

As a final check of the consistency of our model and of the zero width approximation used in Section 2, we have verified that the complete FMSR are nicely satisfied, i.e., the difference of the theoretical and experimental curves (solid curves) in Figs. 2a and 2b multiplied by $\nu d\nu$ and integrated from $M = M_p$ to $M = 2$ GeV, approximately vanishes. This was to be expected from the way the PPR term was determined, along with the approximate equality of the theoretical and experimental backgrounds.

4. The ISR Data and the PPP Coupling

We turn now to the ISR data of ref. 19. The cross section derived from our model (Eqs. (22), (23)), which does not contain any PPP term, is shown in Fig. 4 and Fig. 5 at $p_\perp = 0.9$. The agreement in the nondiffractive region

($x < 0.9$) is quite good indicating that the scaling parametrization of the term $S(t, M^2/s)$, which is dominant in this region, is essentially correct. However, in the diffractive region $0.9 < x < 1$, where the PPR (and PPP if it exists) are dominant, we obtain a too small cross section. It can be seen from those figures that in order to approximately reproduce the experimental results at $s = 2000$ one should multiply the PPR term by a factor of 8. With such a factor the duality picture described in Section 2 would be completely destroyed. Worse than that, the PPR contribution alone would be much larger than the $p_{lab} < 30$ GeV/c data for $M \lesssim 2.5$ GeV. (For instance one can see from Fig. 2b that at $M = 1.78$ GeV the PPR term would be 2 - 3 times larger than the data.) The same conclusion is reached from the fit to the $s = 1995$ (GeV^2) results of ref. 19 using a triple Regge model with PPR and RRP terms: this model gives a too large cross section at $p_{lab} = 24$ GeV/c and $M \lesssim 2.7$ (see Fig. 3). Again the contribution of PPR alone is much larger than the data.[20]

The above results lead us to the conclusion that a sizable PPP contribution has to be present. To support this view, we have added to Eq. (22) the following term:

$$0.823 \frac{1}{\pi} |t| G_P^4(t) \frac{s}{M^2} \tag{24}$$

and compared the model with the experimental data. From Figs. 4 and 5 one sees that the agreement is good.[21] The data are only for $|t| > 0.3$ $(GeV)^2$ and therefore there is no support for the factor of $|t|$ in Eq. (24).

The contribution of such a PPP term to the small M region of the 24 GeV/c data is not negligible as one can see from Fig. 3. This seems to contradict the usually assumed duality between the PPP term and the background, since the first is peaked at threshold whereas the second goes to zero. It may, of course, happen that Eq. (24) is not valid in the resonance region ($M < 2.5$ GeV). Another possibility, suggested in ref. 22, is that the PPP term is dual to the resonances whereas the RRP term vanishes. The residue functions $g^P_{PP}(t)$ and $g^R_{PP}(t)$ in our model being very similar (especially in the region of $|t| > 0.3$ $(GeV)^2$ where the ISR data exist), such a possibility is not excluded by our analysis.

Finally we should like to point out that the necessity of a substantial PPP term has also been arrived at in ref. 23 where a measurement of the inclusive reaction $p+p \rightarrow p+X$ from 15 to 200 GeV/c, with both t and M^2/s, kept fixed is presented.

Conclusion

We have presented a model for $pp \rightarrow pX$ inclusive reaction, summarized by Eqs. (22) - (24). Our model is essentially a triple-Regge description containing the PPP, PPR and RRR terms. However, following ef. , an exponential term in M^2/s is introduced instead of an RRP term. It is possible that confining ourselves to the region $s/M^2 > 5 - 10$, we could have had a normal RRP term; however such an exponential form, while reducing to a normal RRP term for $s/M^2 \rightarrow \infty$ and $t \rightarrow 0$, allows a complete description of the data. We find that the duality sum rules relating the PPR term and the diffractively produced resonances works quite well and allows to determine the $g^R_{PP}(t)$ coupling. However the scheme proposed in ref. 22, with the resonances dual to the PPP term and a vanishing PPR term, is not excluded by the data.

We conclude that a PPP term has to be present which accounts for most of the ISR proton spectrum in the diffractive region. Due to a lack of ISR data for $|t| < 0.3$ (GeV)^2 it is not possible to obtain the value of the triple Pomeron coupling at $t=0$.

Although a different description of the proton inclusive spectrum cannot be excluded, we consider that our model gives a simple and quantitative description of the available high energy ($p_{lab} > 14$ GeV/c) and low momentum transfer data, $|t| < 1$ (GeV)^2.

Acknowledgements

We thank M. Kugler and M. S. Chen for useful discussions. One of the authors (A.C.) wishes to thank Prof. S. Drell for the kind hospitality extended to him at SLAC and another (V.R.) is grateful to Prof. R. Nataf for his hospitality at Orsay last summer, during the early stages of this work.

REFERENCES

1. At $p_{lab} < 30$ GeV/c, assuming reasonable values of the PPP coupling, the PPP term can only be seen at small values of M, and thus has not been included in this fit.
2. A. Capella, H. Högaasen and B. Petersson, Orsay 72/73 preprint (July 1972).
3. Ph. Salin and G. H. Thomas, Nucl. Phys. B38, 375 (1972);
   E. D. Berger, Ph. Salin and G. H. Thomas, Phys. Letters 39B, 265 (1972).
4. J. V. Allaby et al., Contribution to the Fourth International Conference on High-Energy Collisions, Oxford, 1972.
5. V. Amaldi et al., CERN preprint (1972).
6. R. M. Edelstein et al., Phys. Rev. 5D, 1073 (1972).
7. G. G. Beznogikh et al., Physics Letters 30B, 274 (1969).
8. P. D. Ting and H. J. Yessian, Physics Letters 35B, 321 (1971);
   R. M. Edelstein, V. Rittenberg, and H. R. Rubinstein, Physics Letters 35B, 408 (1971);
   J. M. Wang and L. L. Wang, Phys. Rev. Letters 26, 1287 (1971);
   P. H. Frampton and P. V. Russkanen, Physics Letters 38B, 78 (1972);
   J. Dias de Deus and W. S. Lam, Physics Letters 38B, 220 (1972).
9. S. D. Ellis and A. I. Sanda, Physics Letters 41B, 87 (1972).
10. A. I. Sanda, Phys. Rev. (to be published);
    M. B. Einhorn, J. Ellis and J. Finkelstein, Phys. Rev. (to be published).
11. H. Harari, Phys. Rev. Letters 20, 1395 (1968);
    P.G.O. Freund, Phys. Rev. Letters 20, 235 (1968).
12. For other parameterizations, such as $\lim_{M^2 \to 0} \nu^{-3/2} \longrightarrow M^{-3}$ the local duality, as described in Section 2(b) does not appear to work. Why the

parameterizations (12a) and (12b) are better than others is a mystery — the necessity of using the variable ν in the FESR for two-body processes is rather mysterious — and the question of whether a parameterization works better than the others in all inclusive processes is an open question.

13. J. H. Schwartz, Phys. Rev. 159, 1269 (1967).

14. No attempt has been made to check whether $R_r(t)$ in Eq. (16) is linked to a singularity at $\alpha(t) \sim 1$ for all values of t. In order to interpret it as a wrong signature fixed pole one has to assume that all the other singularities give rise to the asymptotic Regge behavior used in the FMSR.

15. H. D. I. Abarbanel, Phys. Rev. (to be published).

16. We have verified that the narrow width approximation tends to overestimate g(t) by $10 \sim 20\%$. Therefore we take $g^R_{PP}(t) = 0.84\, g_1(t)$.

17. An alternative parameterization which gives an equally good fit of the data is the following: for the second term in Eq. (22) one takes the result of the fit in the first paper of ref. 1, i.e.:

$$c_1 = 5.7, \qquad c_2 = 0, \qquad \beta(t) = 24.6\, e^{5.37\, t + 2.11\, t^2};$$

the first term in Eq. (22) is replaced by

$$\frac{1}{s}\left(58\, e^{5.16\, t} + 369\, e^{21\, t}\right)\left(\frac{s}{M^2}\right)^{1.04} \nu^{0.41},$$

and the third term is left unchanged.

18. In the region $M > 2.5$ GeV, the contribution of the PPR term is so small that one can safely use the analytic expression (20) in the whole range of t.

19. M. G. Abbrow et al., CERN preprint (1972);

J. C. Sens, Communication to the Batavia Conference (1972).

20. Note that the low and high energy data we are comparing correspond roughly to the same value of the momentum transfer.

21. In the region $x \sim 1$, the points in Figs. 4 and 5 correspond to rather different values of t and therefore the theoretical curve in Fig. 4 at $x \sim 1$ could be raised by slightly changing the t-dependence in Eq. (24).

22. M. B. Einhorn, M. B. Green and M. A. Virasoro, Phys. Letters 37B, 292 (1971).

23. M. Lieberman et al. (preliminary results).

LIST OF FIGURES

1. The residue function $g_1(t)$ computed from the FMSR (Eq. (13a)). The contribution $g_1^i(t)$ of the various resonances computed from local duality Eq. (15a): the nucleon contribution (dashed line), the 1410 enhancement contribution (dashed-dotted line), the sum of the nucleon and the 1910 contributions (+), the 1520 resonance contribution (▲) and the 1690 one (■). The function $g_2(t)$ (Eq. (13b)) as well as $g_2^i(t)$ (Eq. (15b)) are also shown: the sum $g_2^{940} + g_2^{1410}$ (⊕), g_2^{1520} (▲) and g_2^{1690} (●).

2. The proton spectrum at 24 GeV/c and $\theta_{lab} = 37$ mrad, against the momentum of the outgoing proton. The data points are from ref. 4. The curve is computed from Eqs. (22) and (23). The contribution of the PPR term is shown. The dashed line is the result obtained with the triple Regge model of ref. 19, and the line labelled $\alpha(0) = 0.45$ is the contribution of the PPR term of the same reference. The line labelled $\alpha(0) = 0.7$ is the contribution of the same term multiplied by $(s'/100)^{0.25}$. (This amount changes the intercept from $\alpha(0) = 0.45$ to $\alpha(0) = 0.7$ keeping the normalization at $s = 2000$ $(GeV)^2$ and $x = 0.95$ unchanged.) Finally the line $\alpha(0) = 1$ is the contribution of the PPP term of Eq. (24).

3. The cross section $d\sigma/dtdM$ computed from Eqs. (22) and (23) (dotted line) and from the parametrization in footnote 17 (solid line) as compared to the experimental data of ref. 5: (a) at $\theta_{el} = 15$ mrad, and (b) $\theta_{el} = 27$ mrad. The dashed-dotted line is the experimental background and the dashed line the theoretical one (sum of the first two terms in Eq. (22) with the parametrization in footnote 17). The theoretical curves as determined by the high M fit of the data of ref. 3, have been multiplied by 0.9 to match the data of refs. 4 and 5.

4. The ISR results of ref. 19 compared with the theoretical curve obtained from Eqs. (22) and (23) (curve B) and with the one obtained from adding to curve B the contribution of the PPP term of Eq. (24). Curve D is the contribution of the second term of Eq. (22) and curve C the sum of the first to terms in Eq. (22) (with the parameters of Eq. (23)). Curve E is the result obtained with the triple Regge model of ref. 22.

5. The ISR results of ref. 19 at $p_\perp = 0.7$, 0.8, and 0.9 GeV/c compared with the theoretical curve (B) obtained from Eqs. (22) and (23), and with the one obtained by adding to curve B the contribution of the PPP term in Eq. (24) (curve A). Curve D is the contribution of the second term in Eq. (22) and C the sum of the first two terms in Eq. (22) (with the parameters of Eq. (23)).

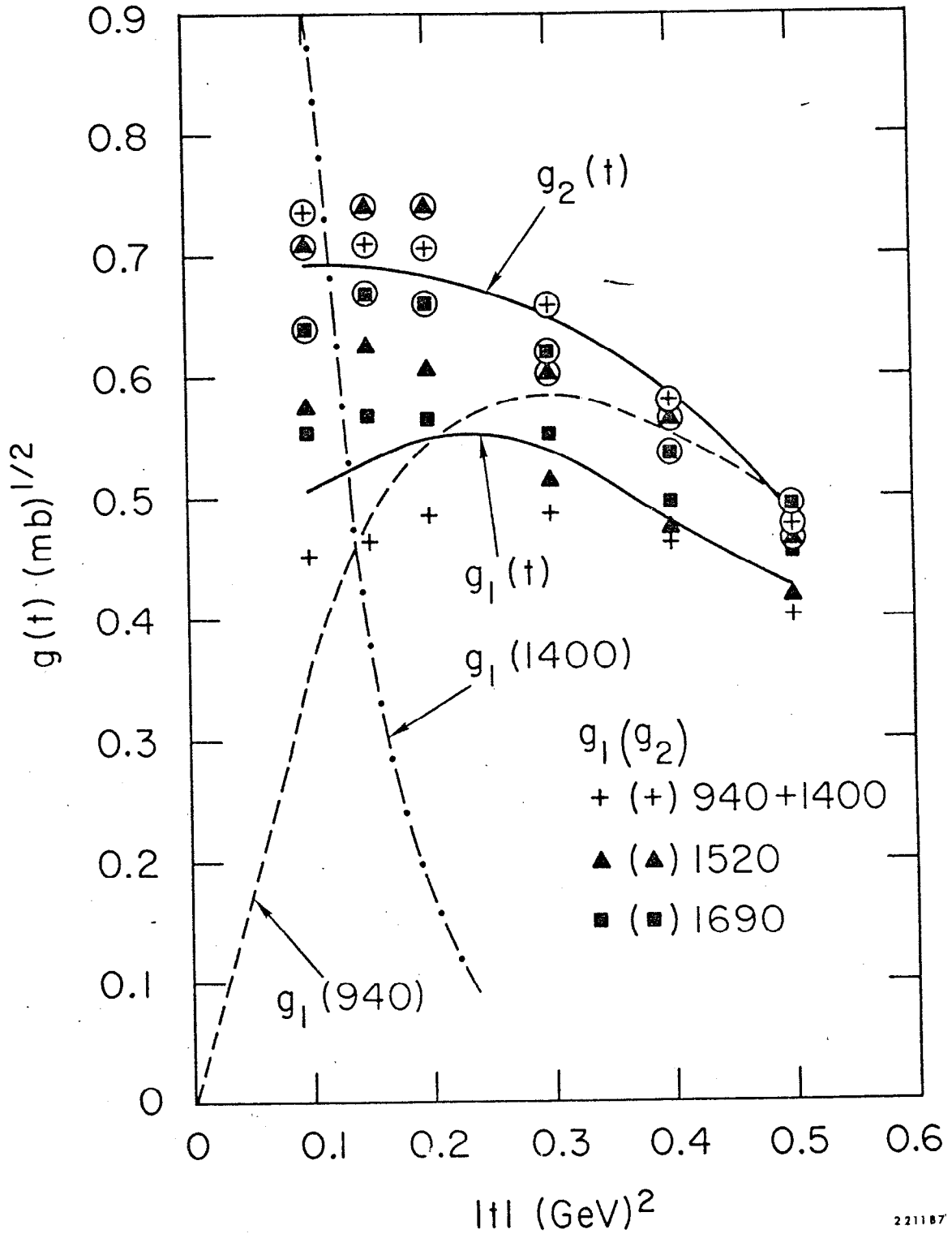
0.9
0.8
0.7
0.6
0.5
0.4
0.3
0.2
0.1
0
g(t) (mb)^1/2
0
0.1
0.2
0.3
0.4
0.5
0.6
|t| (GeV)^2
g2(t)
g1(t)
g1(1400)
g1(940)
g1(g2)
+ (+) 940+1400
▲ (▲) 1520
■ (■) 1690
221187

Fig. 1

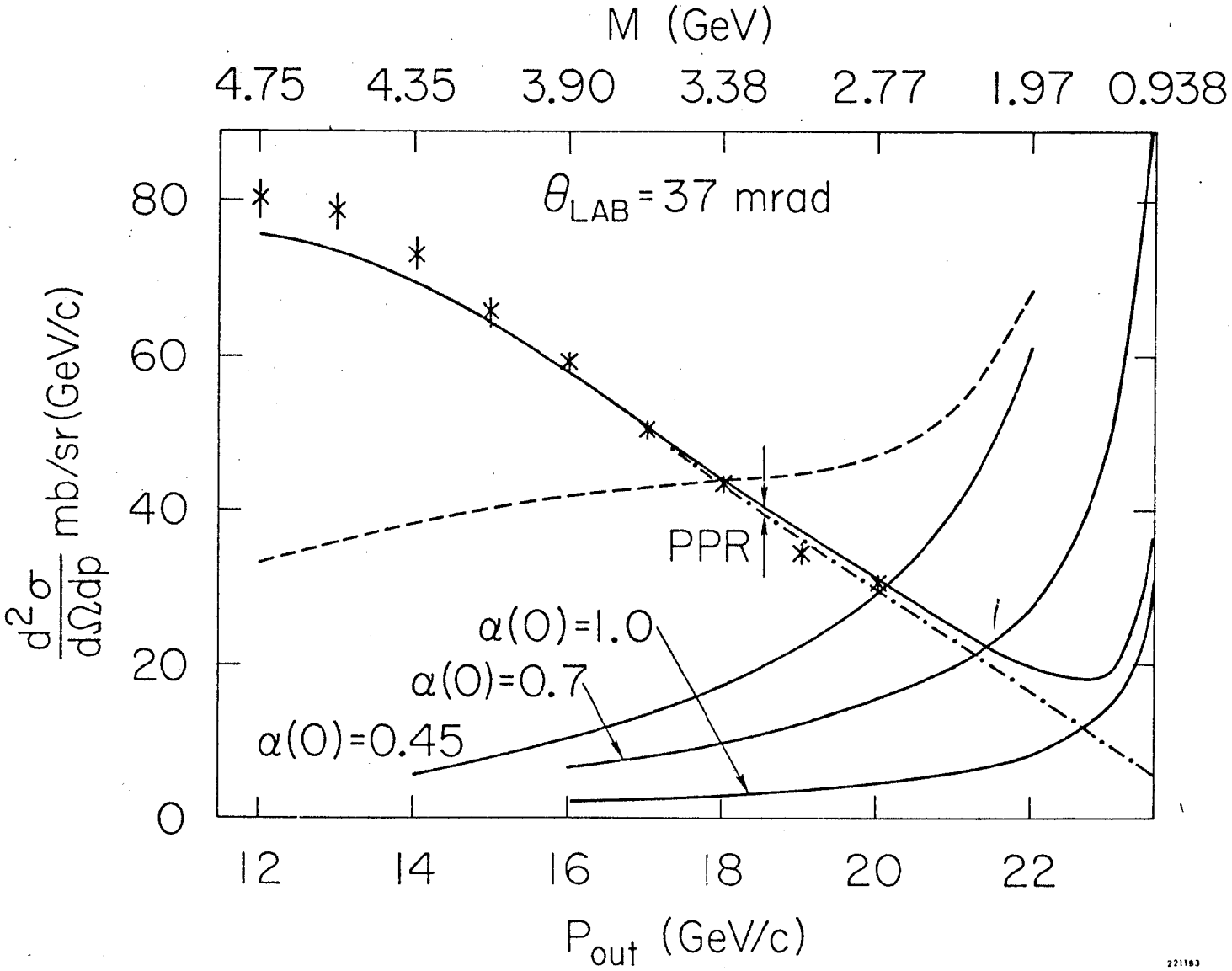
M (GeV)
4.75
4.35
3.90
3.38
2.77
1.97
0.938
θ_{LAB} = 37 mrad
PPR
α(0)=1.0
α(0)=0.7
α(0)=0.45
$\frac{d^2\sigma}{d\Omega dp}$ mb/sr(GeV/c)
80
60
40
20
0
12
14
16
18
20
22
P_{out} (GeV/c)
221183

Fig. 2

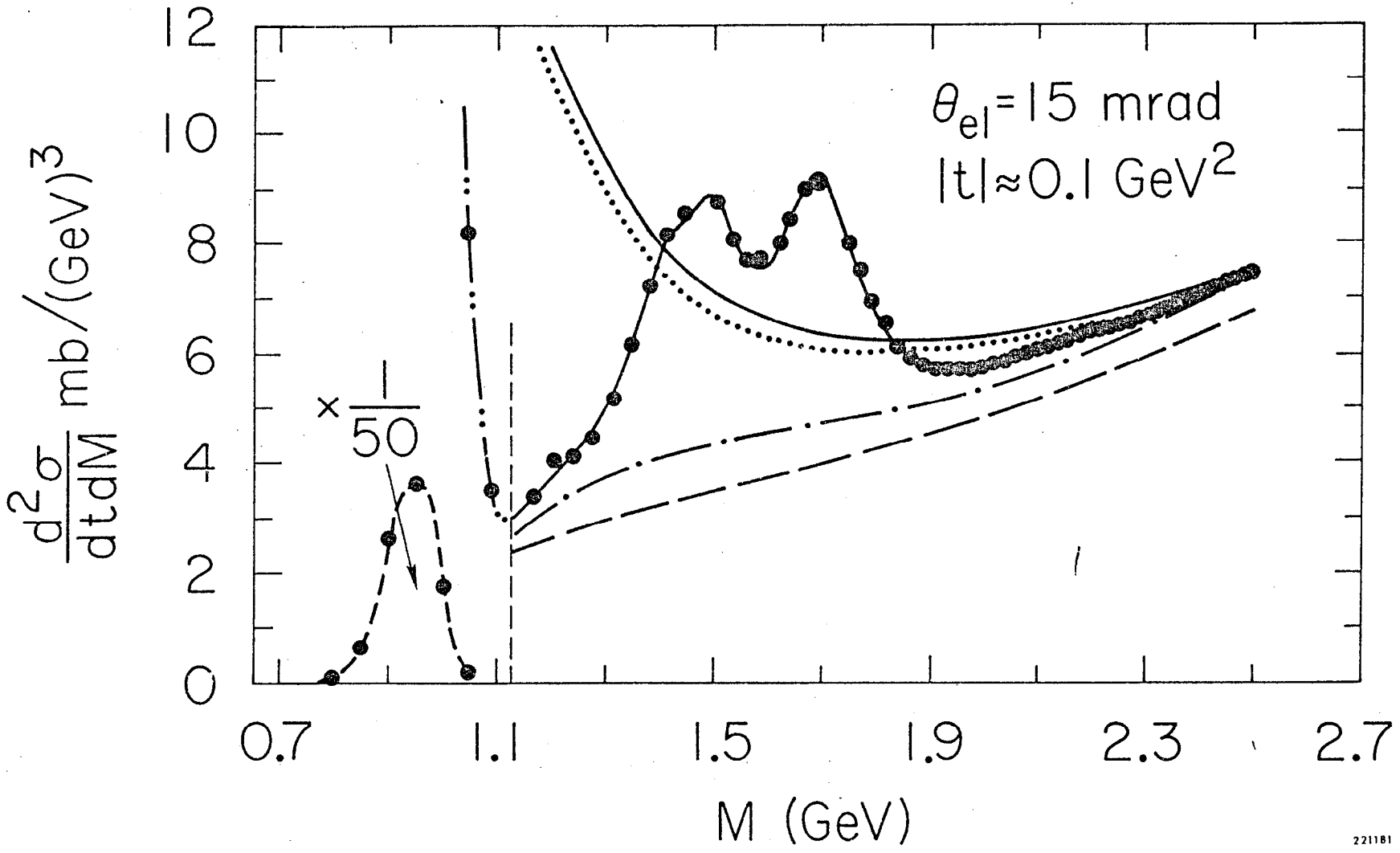
$\frac{d^2\sigma}{dtdM}$ mb/(GeV)^3
12
10
8
6
4
2
0
θ_{el}=15 mrad
$|t|\approx 0.1$ GeV^2
$\times\frac{1}{50}$
0.7
1.1
1.5
1.9
2.3
2.7
M (GeV)
221181

Fig. 3A

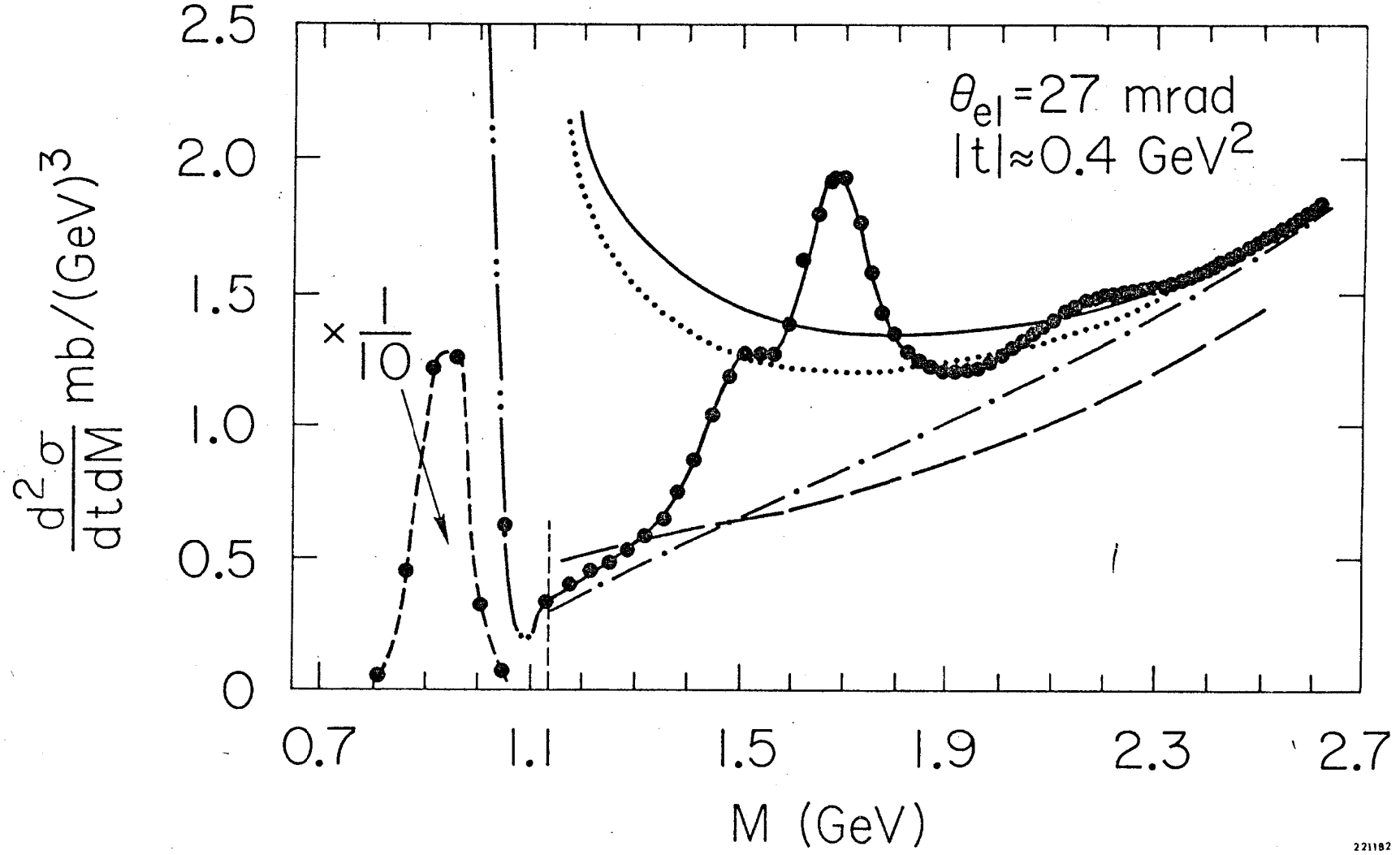
$\frac{d^2\sigma}{dtdM}$ mb/(GeV)^3
2.5
2.0
1.5
1.0
0.5
0
$\times \frac{1}{10}$
θ_{el}=27 mrad
$|t| \approx 0.4$ GeV^2
0.7
1.1
1.5
1.9
2.3
2.7
M (GeV)
221182

Fig. 3B

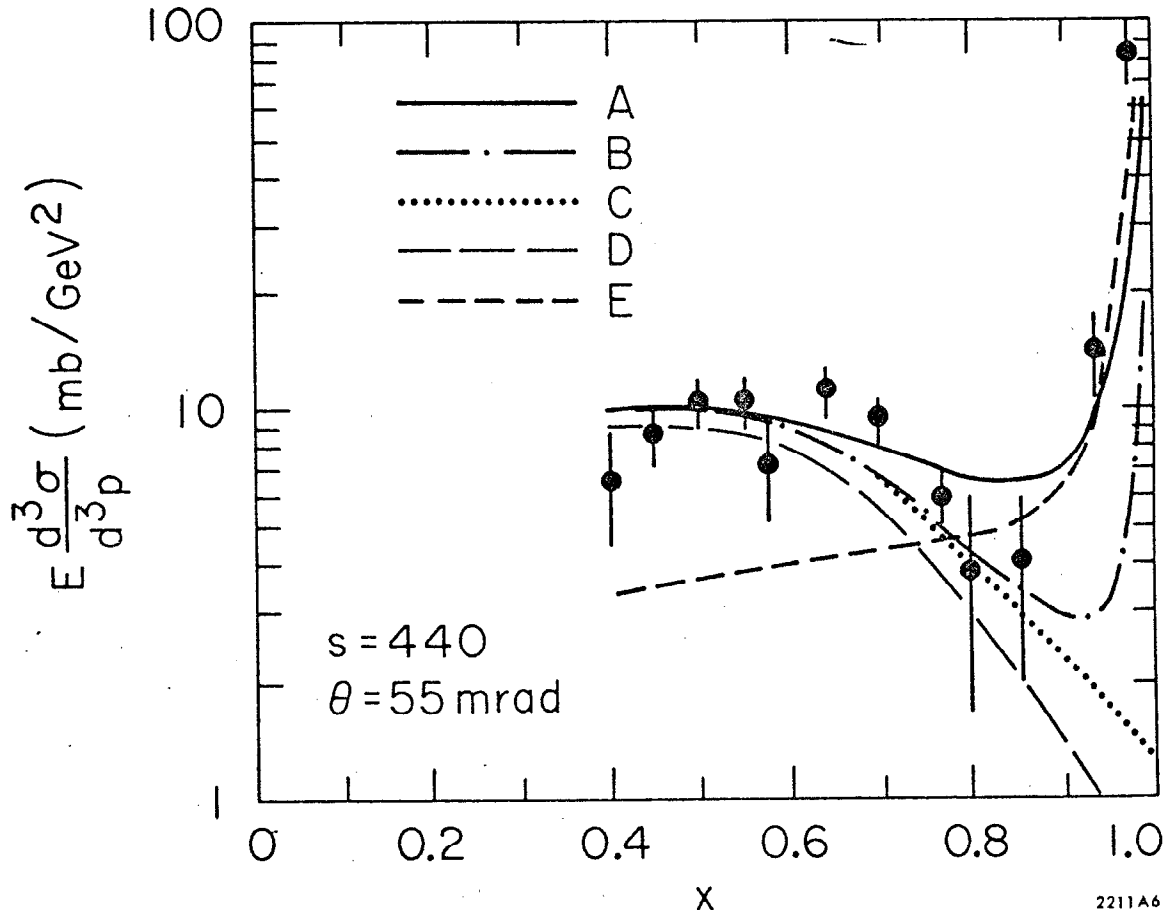
100
10
1
0
0.2
0.4
0.6
0.8
1.0
x
A
B
C
D
E
s = 440
θ = 55 mrad
E d³σ/d³p (mb/GeV²)
2211A6

Fig. 4

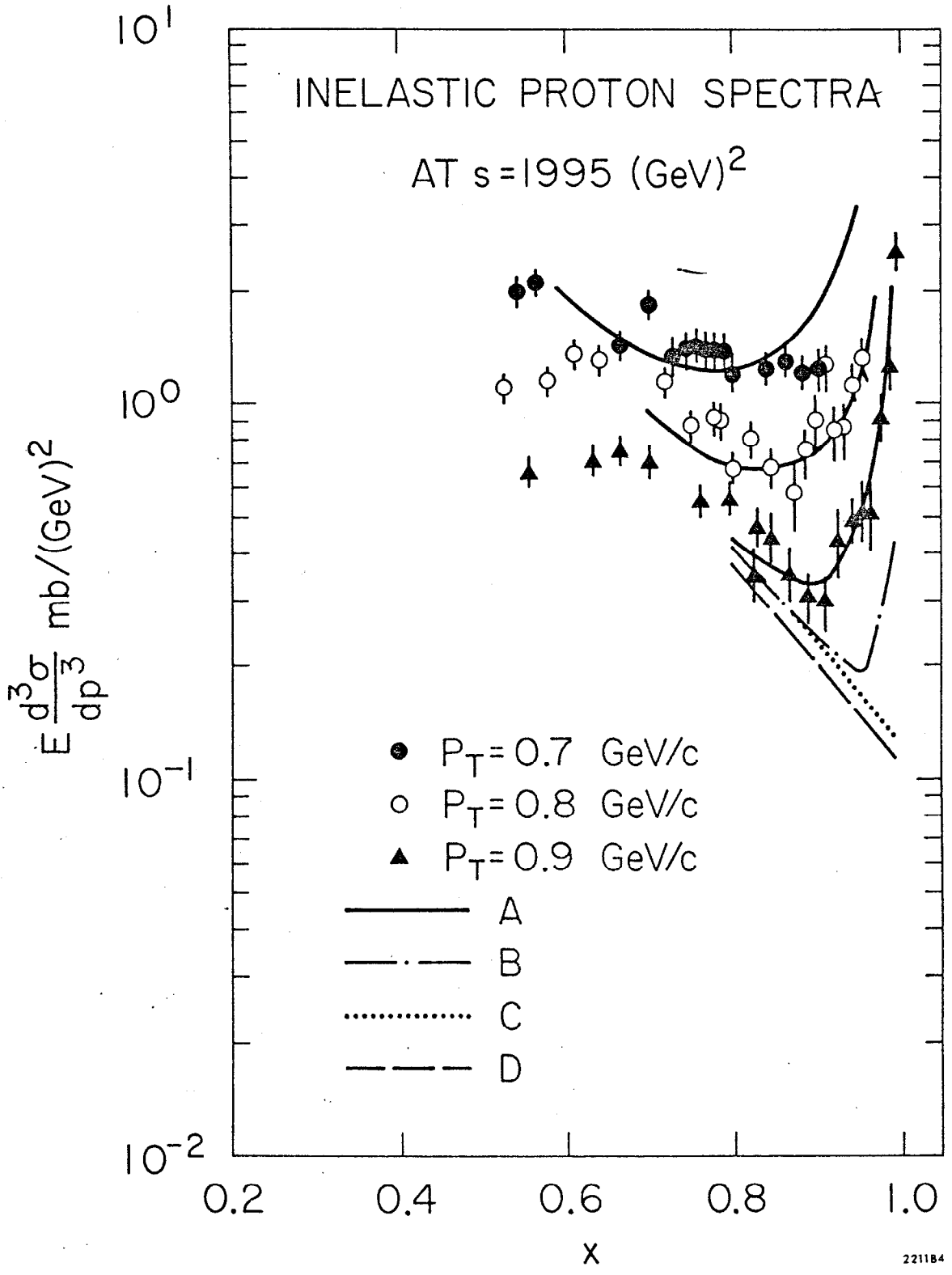
INELASTIC PROTON SPECTRA
AT s=1995 (GeV)^2
$E\frac{d^3\sigma}{dp^3}$ mb/(GeV)^2
10^1
10^0
10^{-1}
10^{-2}
0.2
0.4
0.6
0.8
1.0
x
P_T= 0.7 GeV/c
P_T= 0.8 GeV/c
P_T= 0.9 GeV/c
A
B
C
D
221184

Fig. 5